Physicochemical properties and application of concentrated $KN(SO_2F)_2$/sulfolane solution in high-voltage high-power K-ion batteries

Daisuke Igarashi,[a] Ryoichi Tatara,[a] Satoshi Yasuno,[b] and Shinichi Komaba[a]*

[a]Department of Applied Chemistry, Tokyo University of Science, Shinjuku, Tokyo, 162-8601, Japan

[b]Japan Synchrotron Radiation Research Institute (JASRI), Sayo-gun, Hyogo 679-5198, Japan

Present Address for RT: Department of Chemistry and Life Science, Yokohama National University, Yokohama, Kanagawa, 240-8501, Japan

* Corresponding author

E-mail: komaba@rs. tus.ac.jp

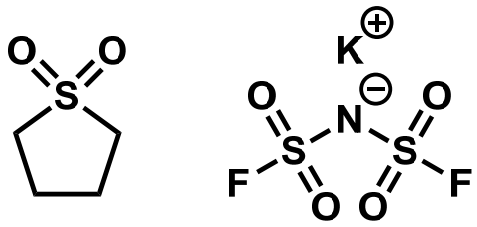

Fig. S1. Chemical structures of sulfolane (SL) and potassium bis(fluorosulfonyl)amide (KFSA)

Table S1. Physicochemical properties of the KFSA/SL = 1/n (mol/mol) solutions

n	Concentration / mol dm^{-3}	Density / g cm^{-3}	Viscosity / mPa s	Conductivity / mS cm^{-1}
1	5.11	1.733	1848	0.255
1.5	4.11	1.642	599.7	0.572
2	3.44	1.579	310.8	0.923
3	2.59	1.503	128.1	1.538
4	2.08	1.456	76.46	1.981
6	1.49	1.403	48.25	2.44
8	1.16	1.373	34.66	2.58
10	0.95	1.354	29.39	2.55
20	0.50	1.313	20.26	2.05
30	0.34	1.298	17.35	1.611

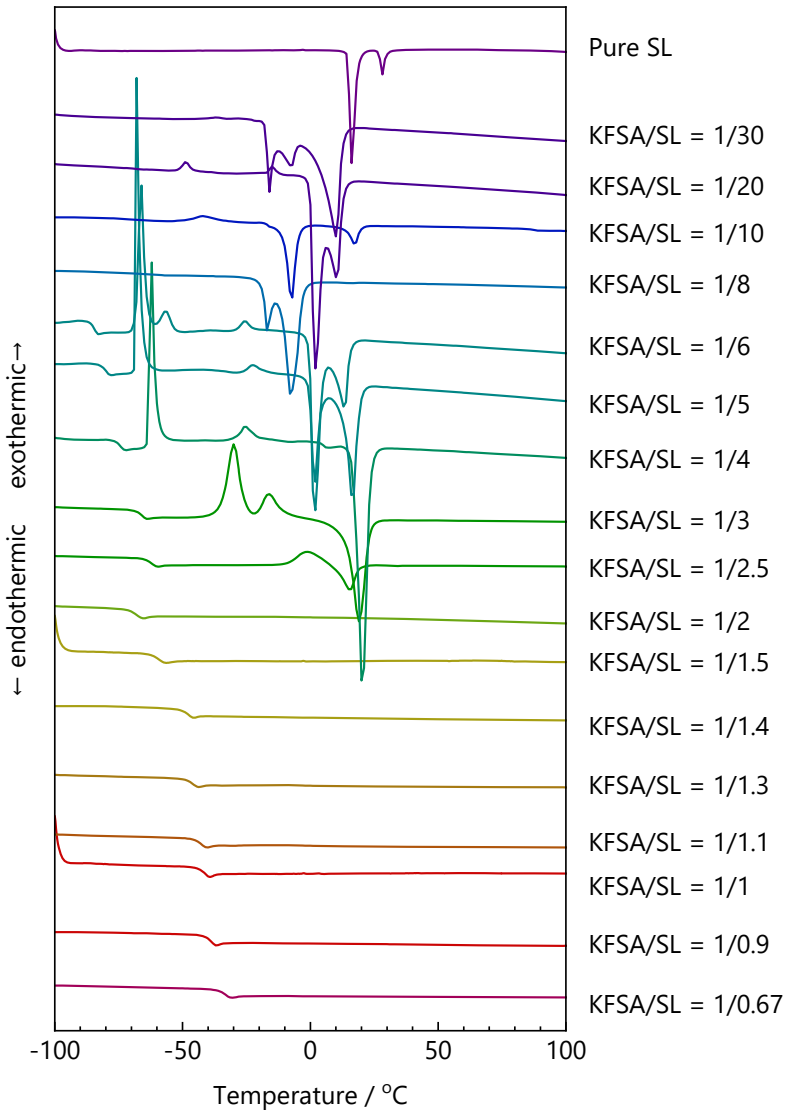

Fig. S2. DSC curves of the KFSA/SL = 1/n solutions.

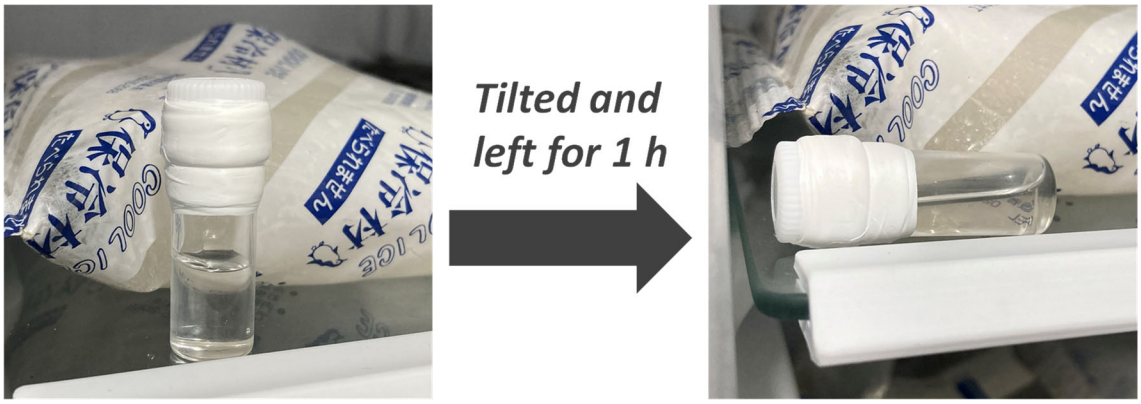

Fig. S3. Photograph of the KFSA/SL = 1/1 electrolyte stored in a freezer for over one year.

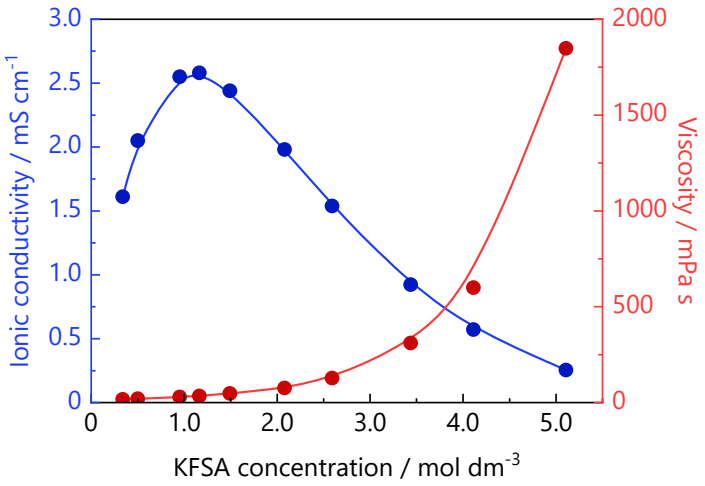

Fig. S4. Ionic conductivity and viscosity of the KFSA/SL = 1/n electrolyte at 25 °C. The measured points were connected using B-spline curves.

Table S2. Physicochemical properties of KFSA/G3 = 1/1 and 1 mol dm^{-3} KPF_6 / EC:PC

Electrolyte	Concentration / mol dm^{-3}	Density / g cm^{-3}	Viscosity / mPa s	Conductivity / mS cm^{-1}
KFSA/G3 = 1/1	3.54	1.406	212.0	0.909
1 mol dm^{-3} KPF_6 / EC:PC	1	1.363	5.885	8.20

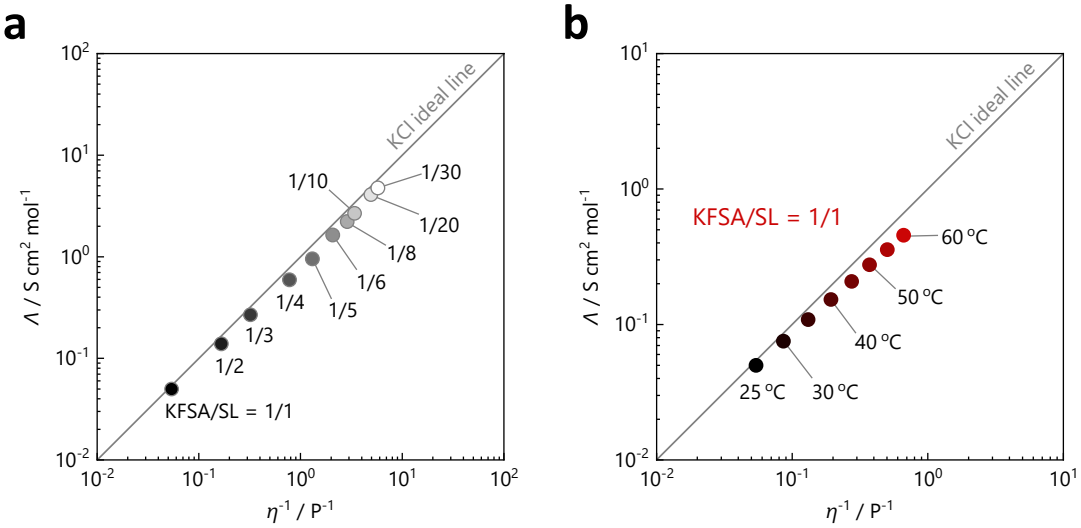

Fig. S5. Walden plots of the (a) KFSA/SL = 1/n solutions with different mixing ratios and (b) KFSA/SL = 1/1 solution at different temperatures.

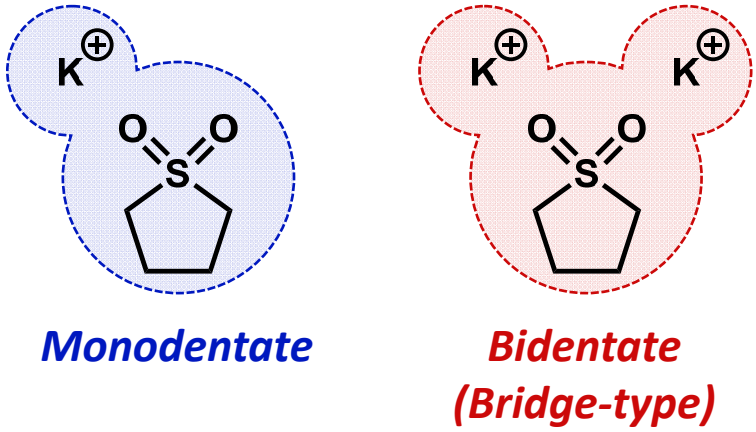

Fig. S6. Schematic of K^+/SL in monodentate and bidentate solvation structures.

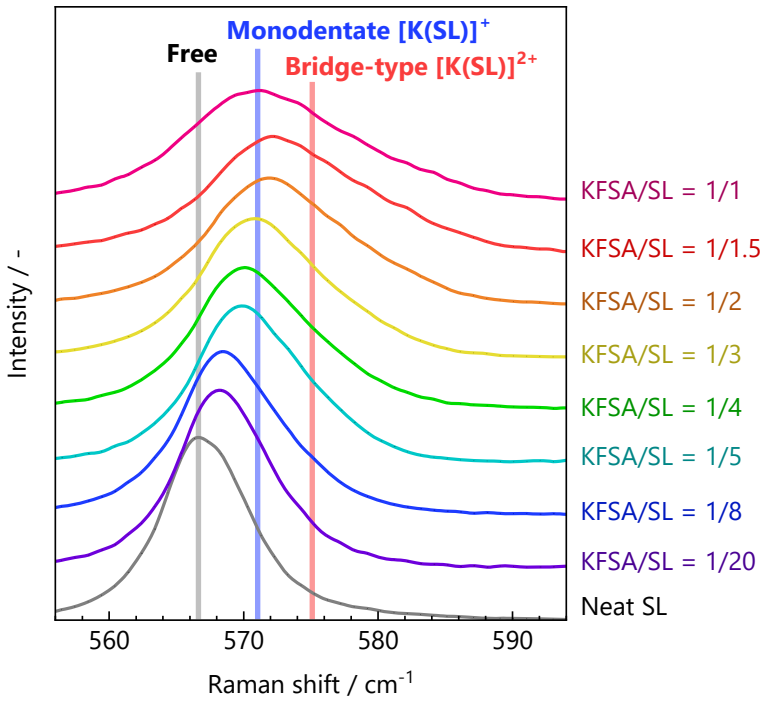

Fig. S7. Raman spectra of the KFSA/SL = 1/n solutions.

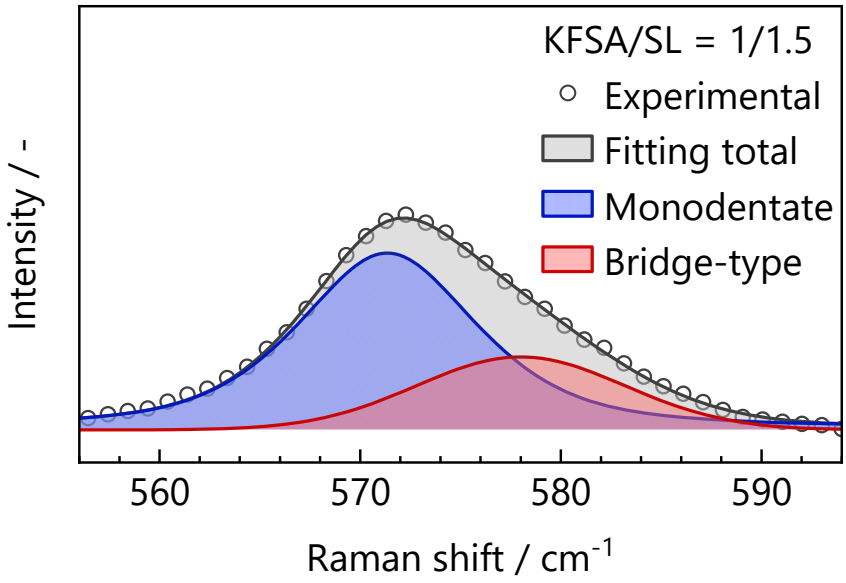

Fig. S8. Deconvoluted Raman spectrum of the KFSA/SL = 1/1.5 solution.

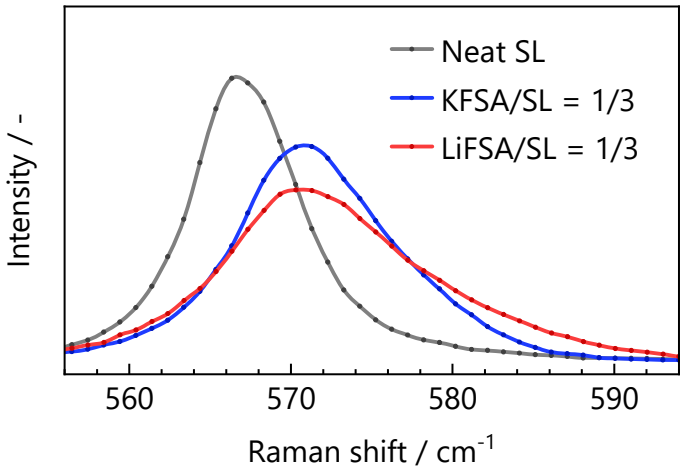

Fig. S9. Raman spectra of the neat SL, KFSA/SL = 1/3, and LiFSA/SL = 1/3 solutions.

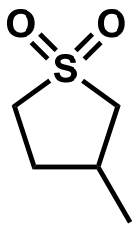

Fig. S10. Chemical structure of 3-methylsulfolane.

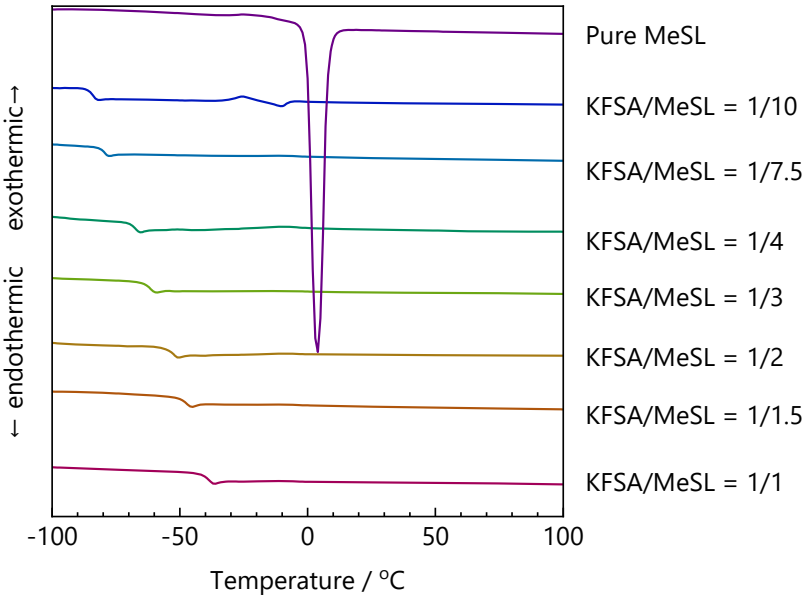

Fig. S11. DSC curves of the KFSA/MeSL = 1/n solutions.

Table S3. Physicochemical properties of the XFSA/SL = 1/1 solutions

Cation (X)	Concentration / mol dm^{-3}	Density / g cm^{-3}	Viscosity / mPa s	Conductivity / mS cm^{-1}
Li	4.91	1.578	2396	0.202
Na	Inhomogeneous mixture of liquid and precipitates			
K	4.68	1.655	2447	0.159

Table S4. Physicochemical properties of the XFSA/SL = 1/1.5 solution

Cation (X)	Concentration / mol dm^{-3}	Density / g cm^{-3}	Viscosity / mPa s	Conductivity / mS cm^{-1}
Li	3.85	1.496	747.6	0.444
Na	3.82	1.546	1533.0	0.0621
K	3.70	1.554	780.4	0.348

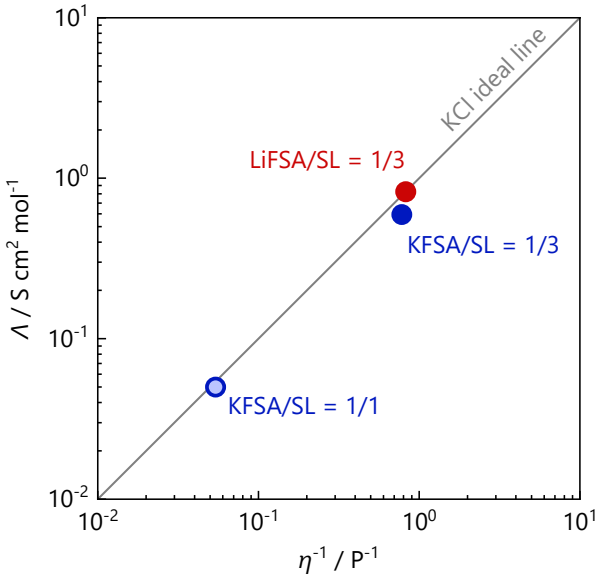

Fig. S12. Walden plots for the KFSA/SL = 1/1, KFSA/SL = 1/3, and LiFSA/SL = 1/3 solutions.

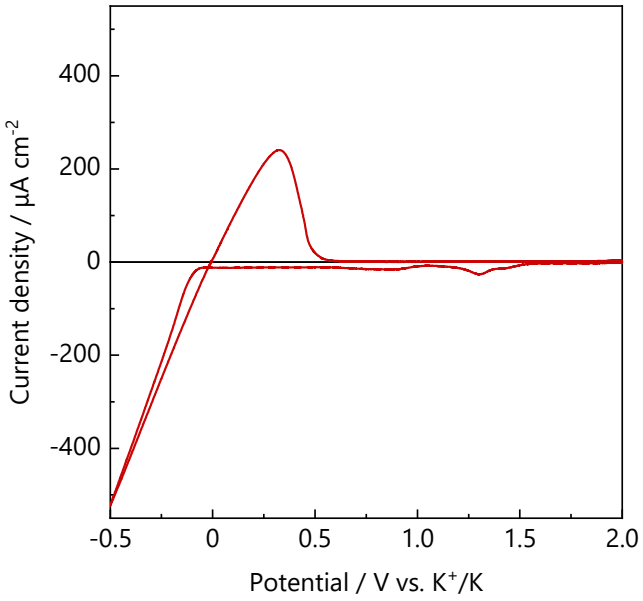

Fig. S13. Cyclic voltammogram of the Cu foil in the KFSA/SL = 1/1 electrolyte measured using a three-electrode cell. The counter and reference electrodes were an activated carbon–acetylene black–polyvinylidene difluoride composite and a potassium metal wire, respectively.

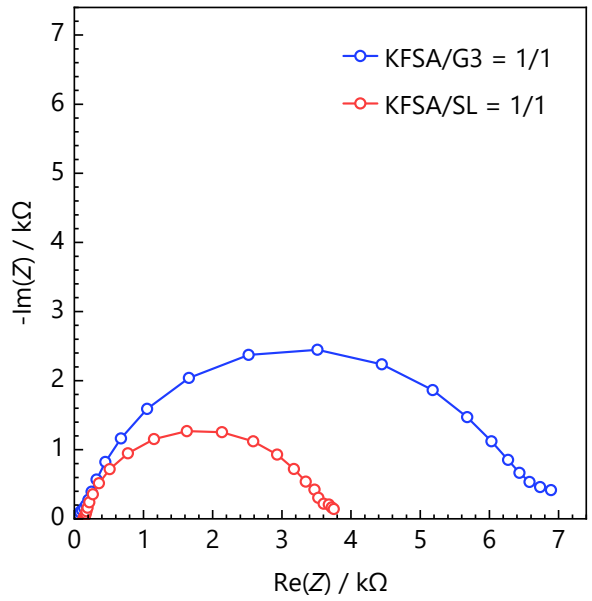

Fig. S14. Nyquist plots of the electrochemical impedance spectra of K//K symmetric cells with the KFSA/G3 = 1/1 and KFSA/SL = 1/1 electrolytes.

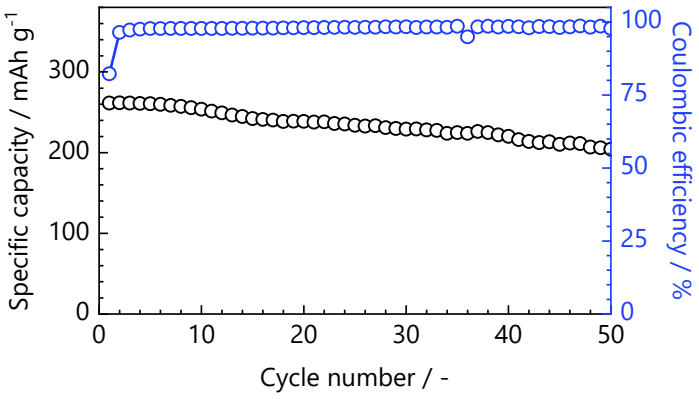

Fig. S15. Cycling performance and Coulombic efficiency of the graphite//K cell with the KFSA/SL = 1/1 solution.

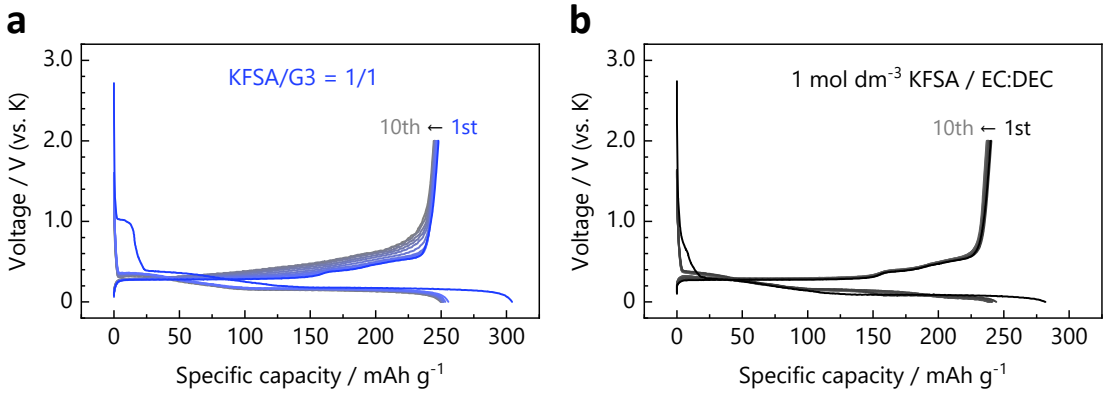

Fig. S16. Charge–discharge curves of the graphite electrodes in the (a) 1 mol dm^{-3} KFSA/EC:DEC and (b) KFSA/G3 = 1/1 electrolytes.

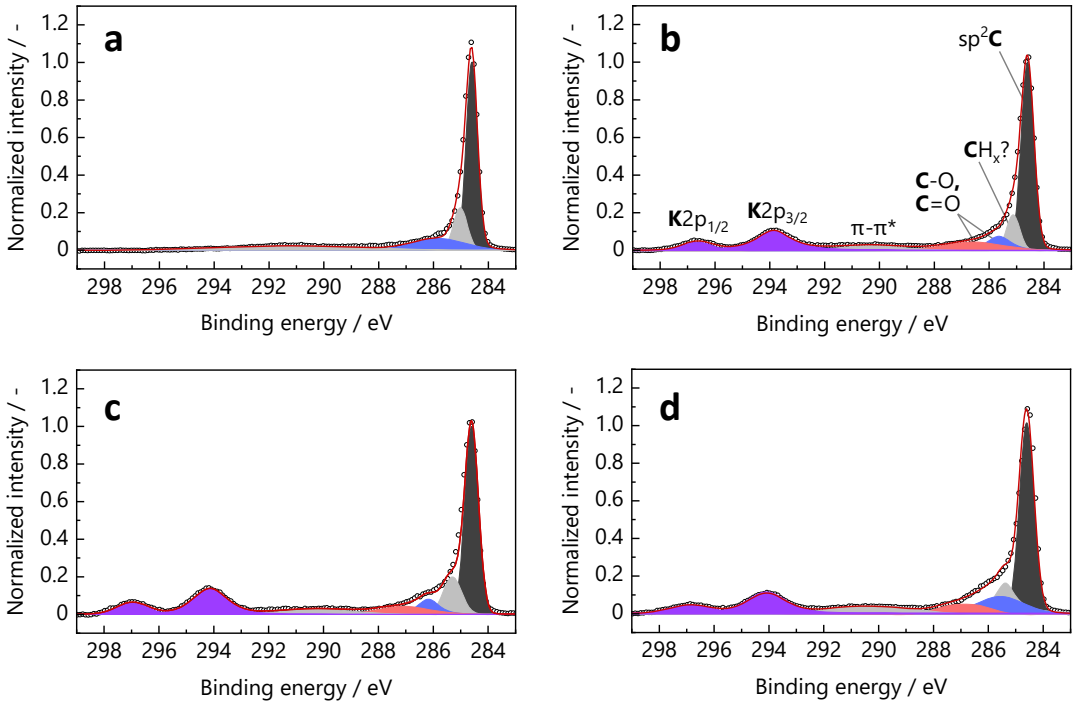

Fig. S17. HAXPES profiles of the graphite electrodes (a) before and after cycling in the (b) KFSA/SL = 1/1, (c) KFSA/G3 = 1/1, and (d) 1 mol dm^{-3} KFSA/EC:DEC electrolytes.

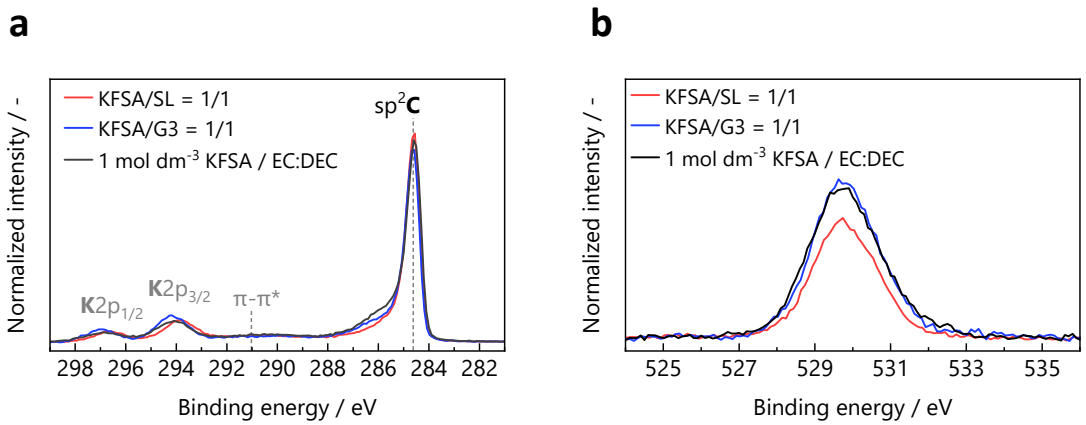

Fig. S18. (a) C 1s and (b) O 1s HAXPES profiles of the graphite electrodes cycled in the KFSA/SL = 1/1, KFSA/G3 = 1/1, and 1 mol dm^{-3} KFSA/EC:DEC electrolytes. (a) shows the overlapping of the spectra shown in Figs. S17b–d.

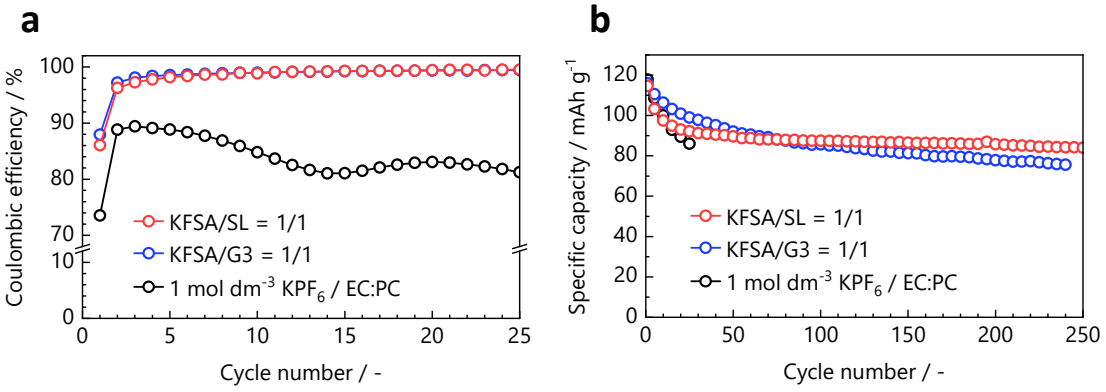

Fig. S19. (a) Coulombic efficiency and (b) long-term cycling performance of the $K_2Mn[Fe(CN)_6]$ electrodes.

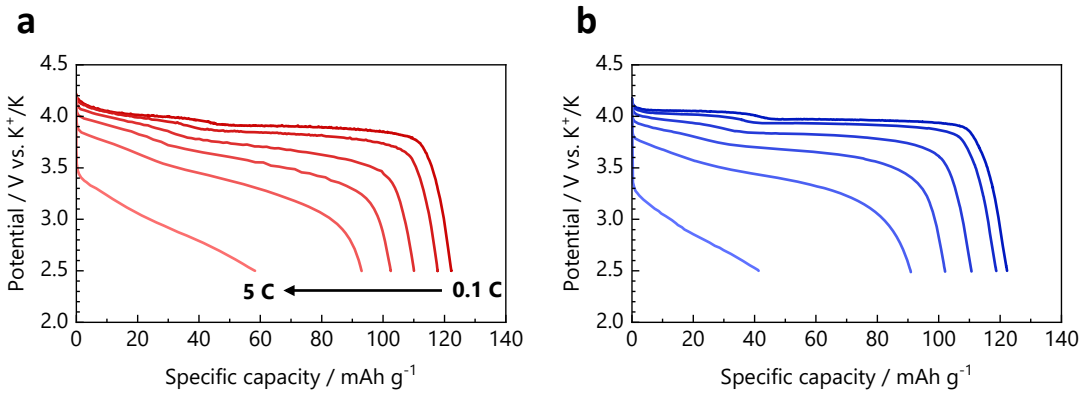

Fig. S20. Discharge rate curves of the $K_2Mn[Fe(CN)_6]$ electrodes at different current densities.

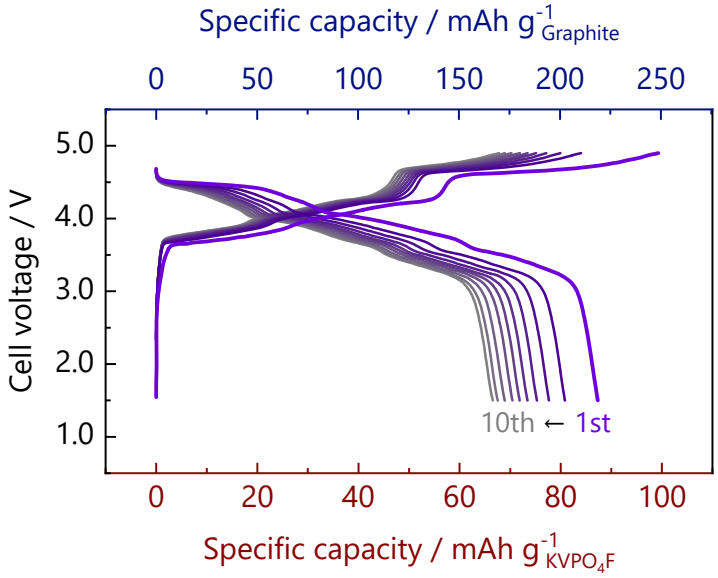

Fig. S21 Charge–discharge curves of the $KVPO_4F$ | KFSA/SL = 1/1 | graphite full cell.

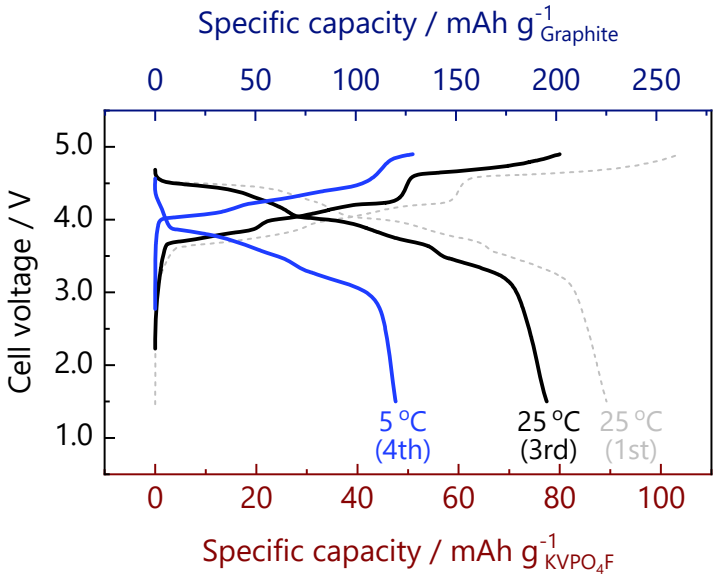

Fig. S22 Charge–discharge curves of the $KVPO_4F$ | KFSA/SL = 1/1 | graphite full cell operated at 25 °C for 1st – 3rd cycle and 5 °C for 4th cycle.